INTERNATIONAL JOURNAL OF AUTOMOTIVE AND MECHANICAL ENGINEERING (IJAME)
ISSN: 2229-8649 e-ISSN: 2180-1606
VOL. 17, ISSUE 3, 8086 – 8095
DOI: https://doi.org/10.15282/ijame.17.3.2020.02.0606

ORIGINAL ARTICLE

Fatigue Crack Growth and Fracture Toughness in a Dual Phase Steel: Effect of Increasing Martensite Volume Fraction

C. Pérez-Velásquez[1,2], D. Avendaño-Rodríguez [1], C. Narvaez-Tovar[2], L. Mujica Roncery[3], and R. Rodriguez-Baracaldo[1]

[1]Grupo de Investigación IPMIM, Universidad Nacional de Colombia, Bogotá D.C. Colombia
Phone: +5713165000 (11214,11203)
[2]Grupo de Investigación GNUM, Universidad Nacional de Colombia, Bogotá D.C. Colombia
[3]Grupo de Investigación en Materiales Siderúrgicos e INCITEMA, Universidad Pedagógica y Tecnológica de Colombia, Boyacá, Colombia

ABSTRACT – Crack growth resistance in dual-phase steel was studied. The dual phase steel microstructure was modified through heat treatments to increase the martensite volume fraction from 10% to 40%. The as-received and heat-treated samples were evaluated using a uniaxial tensile test, fatigue crack growth test, and fracture toughness test. Extended Finite Element Method (XFEM) was used to simulate the crack growth in compact tension test specimens. The results showed that an increase in martensite volume fraction is an effective way to increase the fracture resistance under different load conditions, quasistatics and dynamic, increasing the fracture toughness, tensile strength and fatigue resistance of the heat-treated material. Presence of a highest content of martensite results in formation of an important number of secondary cracks during the fatigue crack growth, which slow down the crack propagation. Moreover, martensite generates a crack closure over the crack tip, making the propagation difficult due to the irregularities caused by the crack growth on the martensite. Finally, the computational load-displacement curves are in good agreement with the experimental data.

ARTICLE HISTORY
Revised: 17th July 2020
Accepted: 7th Sept 2020

KEYWORDS
Dual-phase steel; Fracture toughness, XFEM; Crack fatigue growth

INTRODUCTION

Dual-phase steels are characterised by a high initial hardening capacity and a good ductility to strength ratio, which provides an excellent energy absorption capacity [1–5]. A soft ferrite matrix about which a second dispersed hard phase, generally martensite, is found in its microstructure. It can be obtained through a heat treatment that begins with an inter critical annealing to generate a ferrite-austenite microstructure, followed by a rapid cooling process (quenching), which allows the austenite to martensite transformation [6]. The final properties of the material depend on a set of factors like martensite volume fraction and carbon content, and grain size on each phase, among others, which are principally affected by the steel chemical composition [7].

The main application fields for the dual-phase steel material are the automotive industry and the manufacturing of structures, where good fatigue behaviour is required, complying with high safety standards. Fatigue is the main cause of failures in automotive and machine elements due to the stress fluctuations during their service; therefore, this is an important parameter to consider in the design of this kind of components. However, the research concerned with the fatigue crack growth behaviour has been rarely reported, as is also the case of this kind of study for dual-phase steel. The number of study related to crack initiation and crack growth resistance on the dual-phase steels is increasing, and different works discuss the influence of the microstructure over the fatigue crack propagation. Several authors [8–11] conclude that the increase of the ferrite phase increases the fatigue crack growth velocity; thus, a high martensite content is favourable for this type of steel under fatigue loads. While Idris et al. [12] observed the opposite behaviour; increasing the martensite content rises the fatigue crack growth velocity.

It is well known that the evaluation of fracture toughness in thin sheets is experimentally difficult, mainly for thickness below 3 mm in metals. For thinner samples, exist a high probability of buckling during the test, and this implies the need to include a pair of sheets on the sides to avoid this issue. Additionally, the thinner the sample, the size is smaller, hindering their manipulation during the test. These constraints generate that in the dual-phase steels has not been widely studied. In general, some researches show results from alternative methods like tensile tests [13], impact tests [14], use of special specimens [15], or more recently the use of new methods, like the essential work of fracture tests [16], [17] instead of the one specified by ASTM 1820 [18] standard, in order to decrease the number of samples and reduce the cost of the test. Most of these researches are focused on the influence of microstructure on the mechanical properties. They have observed that the increment of the martensite volume fraction can improve the fracture toughness in dual-phase steels.

Due to the difficulties of performing fracture toughness tests according to ASTM standards and the need to analyse mechanical parts with complex shapes and under complex loads stages, the computational fracture mechanics has taken significant importance during the last years for fracture mechanics problems. The Extended Finite Element Method

*CORRESPONDING AUTHOR | R. Rodriguez-Baracaldo | ✉ rodriguezba@unal.edu.co

(XFEM) is often used due to its advantages, like the capability of allowing the crack propagation through the elements without the need of remeshing after each time step, reducing the computation cost [19]. Different researches use the XFEM method to evaluate crack propagation in metals to evaluate fatigue and fracture under static loads cases [20-22], and specifically on dual-phase steels [23–25].

This work studies the influence of increasing the martensite volume fraction (MVF) on the fatigue crack growth and fracture toughness of dual-phase steel. The MVF of the as-received material was 10%, which increased to 40% through heat treatment. Uniaxial tensile, fatigue crack growth (FCG), and fracture toughness tests were conducted to evaluate the two different groups of materials: as-received (AR) samples and heat-treated (HT) samples. Finally, the XFEM method was used to simulate crack growth for compact test (CT) specimens, comparing the computational load-displacement curves to the experimental ones.

EXPERIMENTAL PROCEDURE

The as-received material was a DP600 dual-phase sheet with a 3.4 mm thickness. Chemical composition was determined by an optical emission spectrometry obtaining 0.15% C, 1.05% Mn, 0.41% Si, 0.04% S, and Fe (balance). Tension test samples were processed in agreement to ASTM E8 [26], and CT specimens for fracture toughness and fatigue crack growth tests were manufactured according to ASTM 647 [27] and ASTM 1820 [18]. Figure 1 shows the geometry and characteristics of each CT specimen, for which it was used electrical discharge machining (EDM) for machining the notches in order to avoid residual stress on the crack.

The material was heat-treated in a tubular furnace to modify the martensite content in the microstructure of the as-received steel. The material was heated up to 950 °C for 30 min; then it was cooling rapidly in brine (10% concentration). The samples were coated with an oxidation-resistant protective coating to avoid steel decarburisation. The metallographic preparation consists of sandpaper grinding and polishing up to 1 µm, followed by an etching process with Nital reagent, which reveals the specimens microstructure. Posteriority was observed using an optical microscope Olympus LECO IA32 and scanning electron microscope SEM FEI Quanta 200.

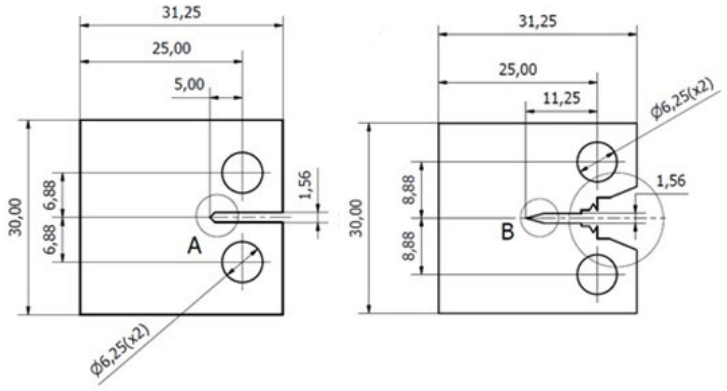

(a) (b)

Figure 1. Compact tension specimens for (a) fatigue crack growth and, (b) fracture toughness.

The fatigue tests were conducted at room temperature using a Baldwin fatigue machine, under load control conditions using a sinusoidal waveform at a frequency of 30 Hz. The ratio of minimum to maximum stress R was 0.1. The crack propagation was measured with DinoLite optical microscope and image analyser. The uniaxial tensile and fracture toughness test were conducted on a Shimadzu 500 KNI universal testing machine. A 25mm Epsilon gauge length extensometer recorded the deformation data for uniaxial tensile test, using a crosshead speed of 1 mm/min at room temperature. An Epsilon gage type clip recorded the displacement for the fracture toughness test. Fracture surfaces were observed in the rolling direction.

NUMERICAL PROCEDURE

Figure 2 shows the geometry of the solid domain, corresponding to a simplified geometry of the CT specimen used on the fracture toughness test. True stress and true strain data were used to determine the elastoplastic properties, as well as the fracture parameters obtained from experimental results. The XFEM model was defined using a traction separation law with maximum principal stress as initiation criterion. The mesh was generated using three- dimensional solid eight-node brick elements with reduced integration. A convergence analysis showed less than 1% error with an element size of 1 mm; therefore, the total number of elements was 7912. Structured and non-structured meshes were used to evaluate the XFEM sensitivity to the mesh.

The pins were modelled as rigid bodies, and surface-to-surface contact was defined between the pins and the specimen holes. A vertical displacement was applied at the top pin while all motions of the bottom pin were restrained. The XFEM enrichment area, where crack propagation is allowed, was defined at the centre zone of the specimen, as shown in Figure 2.

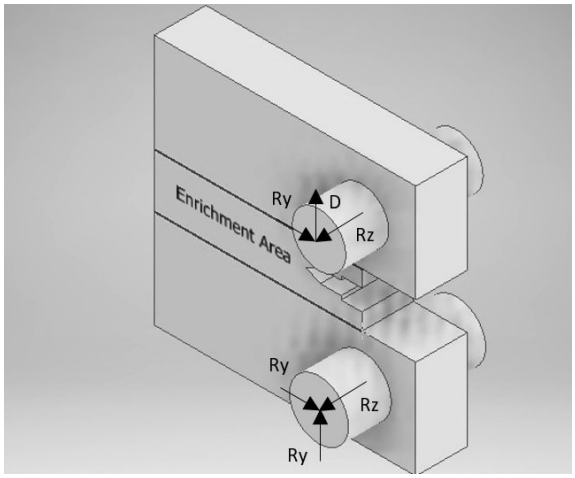

Figure 2. Computational solid domain with defined boundary conditions at the pins, and enrichment area for XFEM

RESULTS AND DISCUSSIONS

Microstructural Characterisation

Figure 3 shows the optical micrographs of AR and HT samples. The AR microstructure showed a homogeneous structure with uniform grain size. Moreover, it shows a clear difference between the two phases, ferrite, and martensite. It is possible to observe that the martensite (black zone) is homogeneously distributed, with 10% MVF (martensite volume fraction). The HT microstructure maintained fine grain size; nevertheless, the grains are less equiaxial compared to the ones found in the AR microstructure, and martensite content increased considerably up to MVF 40%. In this case, the martensite showed a blocky structure, which is typically in dual-phase steels obtained at high inter critical temperature.

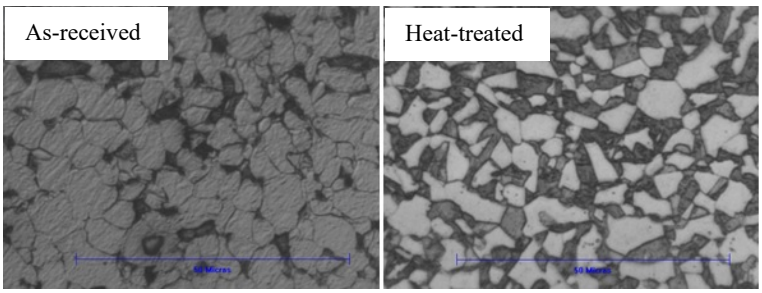

(a) (b)

Figure 3. Optical micrographs of (a) as-received and, (b) heat-treated samples.

Tensile Test

Figure 4 shows the obtained stress-strain curves, while Table 1 summarises the mechanical properties for dual-phase steel. AR samples show continuous yielding and significant difference between the yield strength and ultimate strength, showing the high strain hardening capability of these materials. HT samples show yield strength and the ultimate tensile strength higher than AR material, mainly due to the increase of the martensite phase. Both materials exhibit a rather lower yield strength, which is could due mainly to the fact that the dislocation in coarse ferrite grains leads to cross-slip, inducing to a low strength yield behaviour [28]. It is essential to highlight the presence of plateau in the area of elastic-plastic transition, which is explained by the presence of dissolved carbon that blocks the movement of the dislocations. Generally, with heat-treatments as the one used on this work, it is possible to achieve higher strength values. However, the low carbon content in the as-received steel induces that the martensite has lower strength and hardness compared to dual-phase steels with high carbon content [29]. This behaviour shows that the martensite volume fraction (MVF) is a dominant factor in controlling the strength and ductility of the dual-phase steels. In general, increasing the MVF results in increasing the strength of DP steel and decreasing ductility [30]. However, other researches suggest that the refinement of martensite island or the distribution of fibrous martensite can enhance the ductility of dual-phase steel [28–31]. Therefore it is possible to achieve high strength tensile values and good ductility. This relationship between the strength of dual-phase steel and its MVF has been found linear as reported by Fonstein [32].

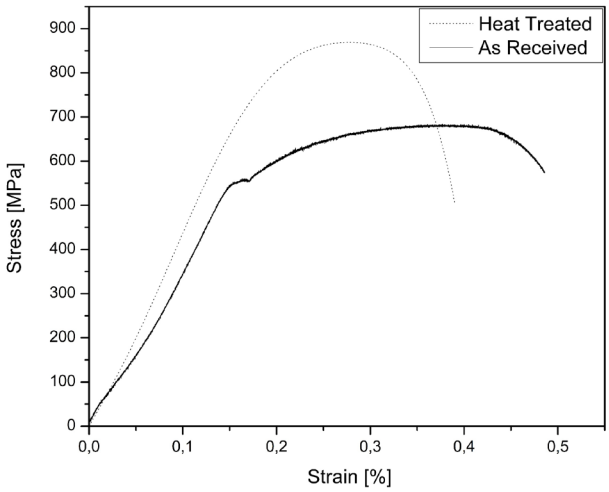

Figure 4. Stress-strain curves for as-received and heat-treated samples.

Table 1: Mechanical properties for as-received and heat-treated samples.

Sample	UTS (MPa)	YS (MPa)	Elongation (%)
AR	682	535	48
HT	873	510	38

Fatigue Crack Propagation Test

Figure 5 summarises the behaviour of the fatigue crack growth for AS and HT materials in terms of the crack growth rate (da⁄dN), and the threshold stress intensity factor ΔK. The results fit quite well to Paris´ law in Eq. (1), where *C* and *m* are the Paris constants. The Paris' law is appropriate to evaluate the crack growth rate in the region II, which generally is the region of most significant interest to predict the fatigue life due to it's relatively no sensibility to the microstructure and its stable crack growth.

$$\frac{da}{dN} = C\Delta K^m \tag{1}$$

Usually, the results of fatigue crack propagation test show high scattering, which is associated with the own nature of the crack growth phenomenon and the device sensitivity used on the measurement. Thus, the potential data fitting is not good enough to calculate de Paris constants (*C* and *m*). For this reason, the ASTM E647 standard [27] recommends performing a statistical treatment on the data to decrease scattering and obtain more accurate values. This work uses the model proposed in reference [33] for data fitting,

Figure 5 shows that the range of stress intensity factor is 17-30 MPa $m^{1/2}$ for AR samples and 18-30 MPa $m^{1/2}$ for HT samples, which means that both materials are in the same range of ΔK. The results showed that the HT samples have a higher crack propagation resistance compared to the AR samples. Therefore, a microstructure with higher martensite content increases the fatigue crack propagation resistance. The AR samples require an average of 27000 cycles to reach the unstable crack growth, while the HT samples require about 45000 cycles. This phenomenon is mainly due to the hard element present in the microstructure [34], that for this case is the higher martensite content in the microstructure. Martensite can generate crack closure over the crack tip and difficulting crack propagation, due to the irregularities caused during the crack propagation on the martensite surface. Table 2 listed Paris constants for AR and HT samples: HT samples have higher values for the *m* parameter and a lower value for *C* parameter when compared to AR samples. This indicates the increase of fatigue crack resistance. A similar phenomenon was reported by other authors; Laurito et al. [35] mention that in the heat-treated conditions, the harder phases scattered over the softer ferritic phase, thus creating a tendency if the crack to deviate from these phases and to propagate principally through the ferrite, resulting in a more complex crack path, decreasing the fatigue crack growth velocity, Akay et al. [36] shows that increasing of harder phase (martensite) on low carbon steel results in an increase of fatigue life, Idris et al. [37] mentions that when the martensite volume fraction increases, there is more possibility that the cracks find martensite islands on their way, which makes the crack path much difficult, decreasing the crack propagation velocity. This is according to the reported by Zhao et al. [38], who mentions that the exists directly the relationship between the fatigue limit and tensile strength, which occurs when increasing in a tensile strength results in an increase on fatigue limit, which is possible achieve when increasing the martensite content in the dual phase steel.

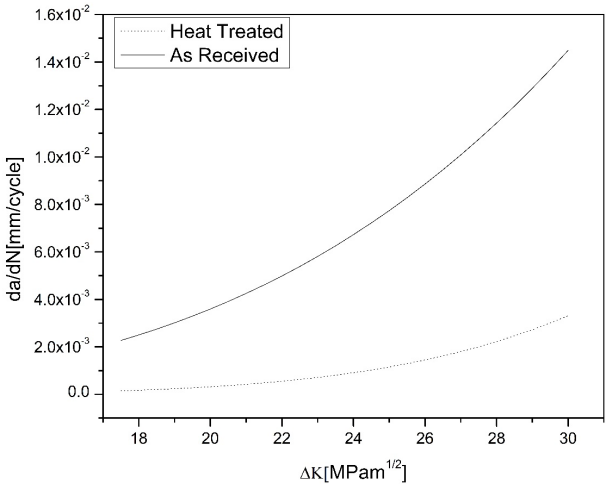

Figure 5. Crack growth rate versus stress mean intensity factor for as-received and heat-treated samples.

Table 2: Paris constants for as-received and heat-treated samples

Sample	*C*	*m*
AR	3.75×10^{-8}	3.67
HT	9.51×10^{-12}	5.78

The obtained values for *C* and *m* parameters can be compared with values reported by [8], which mention these parameters are 8.440×10^{-13} and 5.193 respectively for the material with the higher martensite content; while 4.671×10^{-8} y 2,491 for the as-received material, which contains 16% of martensite. The values and behaviour for the parameters *C* and *m* are very similar since these are in the same magnitude order both for AR material and HT, where the HT contains a higher MVF.

Figure 6 shows the fracture surfaces in the region of crack propagation by fatigue for AR and HT samples; it is possible to notice that the crack growth mechanism is similar for the different percentages of martensite. For both materials, a tortuous path is generally observed, evidencing a propagation of transgranular cracks, where the different peaks and valleys are the product of tension and compression loads. Additionally, it is possible to see patterns of striations over different regions, which are generated by the cyclic loads and represent the extension of the cracks, in theory, the striation is basically a series of parallel, slightly curved curly bands which are perpendicular to the crack growth direction. It is also possible to show a series of secondary cracks on the fracture surface, which are more evident in Figure 6(c) and 6(d) and are related to HT material, which is the material with higher martensite content. The second cracks are responsible for the deceleration of crack growth by dissipation the energy of the crack tip, so the degree of secondary cracking can increase with an increase in martensite content.

Fracture Toughness Test

The procedure specified on the ASTM 1820 standard [18] is used to determine the fracture toughness. Equation 2 was used to calculate the J- Integral value, where the elastic and plastic components, J_{el} and J_{pl}, are determined through Eq. (3) and (4), respectively where *E* is the Elastic Modulus, *v* is the Poisson Ratio, *K* is the stress intensity factor, A_{pl} is the area under the force-displacement curve, η is the geometric factor, *BN* is the thickness of the specimen and b_o correspond to the uncracked ligament. Table 3 presents the J integral results for both materials, and one can see that the HT samples have a slight increment on the fracture toughness.

$$J = J_{el} + J_{pl} \tag{2}$$

$$J_{el} = \frac{K^2(1-\nu^2)}{E} \tag{3}$$

$$J_{pl} = \frac{\eta A_{pl}}{B_N b_0} \tag{4}$$

Table 3: Fracture toughness for as-received and heat-treated samples

Sample	Maximum principal stress (MPa)	Fracture energy (N/mm)	*J* (N/mm)
AR	680	500	500
HT	870	535	550

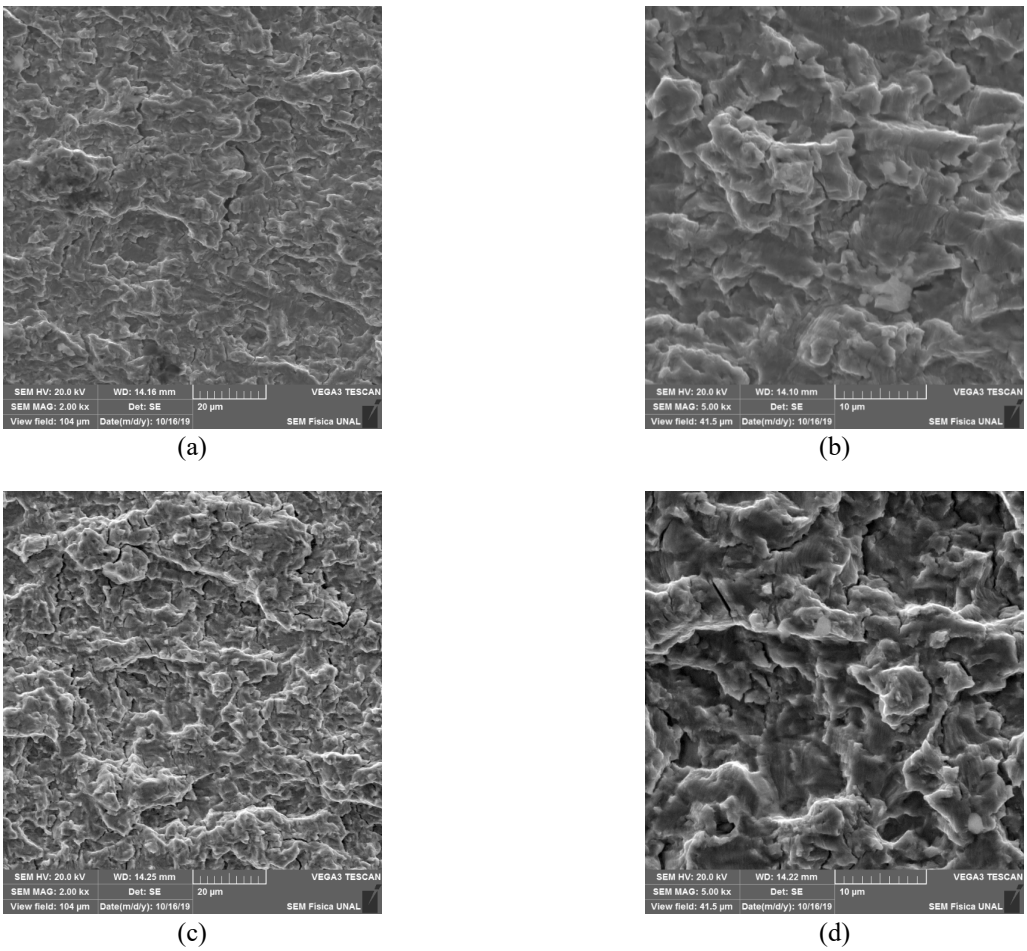

Figure 6. SEM fractographs of crack propagation surface of (a),(b) as-received and, (c),(d) heat-treated fatigue specimens.

The increase of fracture toughness in HT samples could be explained from the correlation between the two microstructural phases. Due to different properties and mechanical behaviours of the ferrite and martensite, a plastic incompatibility occurs during material deformation, in general, locations as sharp corners of the boundaries are considered stress concentrations. This may be the primary reason for micro failures in the microstructure of the dual-phase steel so that locations as the martensite-martensite interface or ferrite-martensite boundaries are common sources of micro failures during the deformation [39]. The fractures occur mainly due to microvoids growth that is generated by the decohesion of the phases because they cannot deform jointly. This phenomenon is mainly observed on low carbon content dual-phase steels [40]. Therefore, it is possible to reach better values of fracture toughness when the phases achieve synergy between them. Generally, this condition is possible when the material microstructure has a similar content of ferrite and martensite. In the case of different content, when the martensite volume fraction increase, the carbon content within this phase is less, increasing their ductility. However, the high content of martensite produces brittle behaviour [41]. According to this, a higher volume fraction of martensite, about 40% in this case for HT samples, could increase their fracture toughness slightly in comparison with AR sample which has less content of martensite, see Figure 7. Additionally, all samples have a low amount of carbon, although the hardness observed on the martensite after the heat treatment is lower than 260 HV. It represents a significant increase when compared with AR samples, which have 197 HV. This hardness suggests a good ductility on the HT samples.

Precisely mention that as well as a good tensile resistant, it is evident in dual-phase steels when the mechanical homogeneity is high, the fracture toughness can improve in the same way. In general, the fracture toughness depends on the microstructural properties. However, it has been found that most refined microstructural characteristics of martensite and ferrite alongside a ferrite-free of any carbide precipitation allows reaching excellent values of fracture toughness [42].

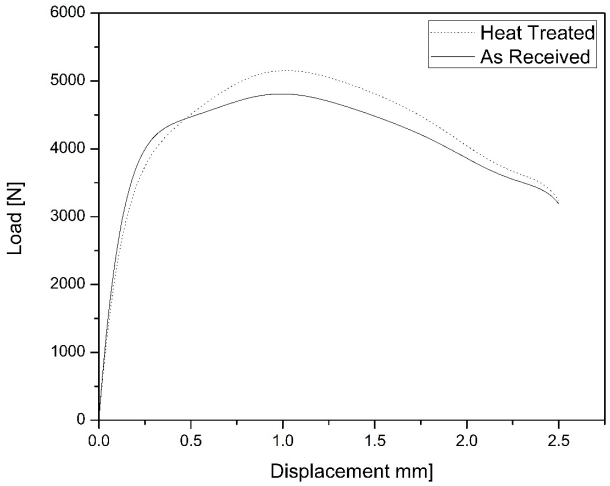

Figure 7. Load-displacement curves at fracture toughness test for as-received and heat-treated samples.

Figure 8 shows the SEM fractography of the fracture surface for AR and HT samples. A ductile type fracture is evident in both materials, which is characterised by the generation of dimples, indicating a rupture occurring by nucleation, growth and coalescence of microvoids, in this case a large number of small dimples and deep holes are observed over the entire fracture surface, this particular distribution of dimples on the fracture surface is common in dual-phase materials that are subjected to elastic-plastic deformation in both phases [43]. However, it is possible to observe that the size of the dimples in AS material is greater than observed in HT material, in which the density of dimples is greater, this generally suggests that this material has a higher tensile strength [44]. This feature is associated with high martensite content since under this condition the low localised deformation before the fracture restrains the coalescence of micro-voids and in this case, the damage is generated by a high micro-void nucleation rate.

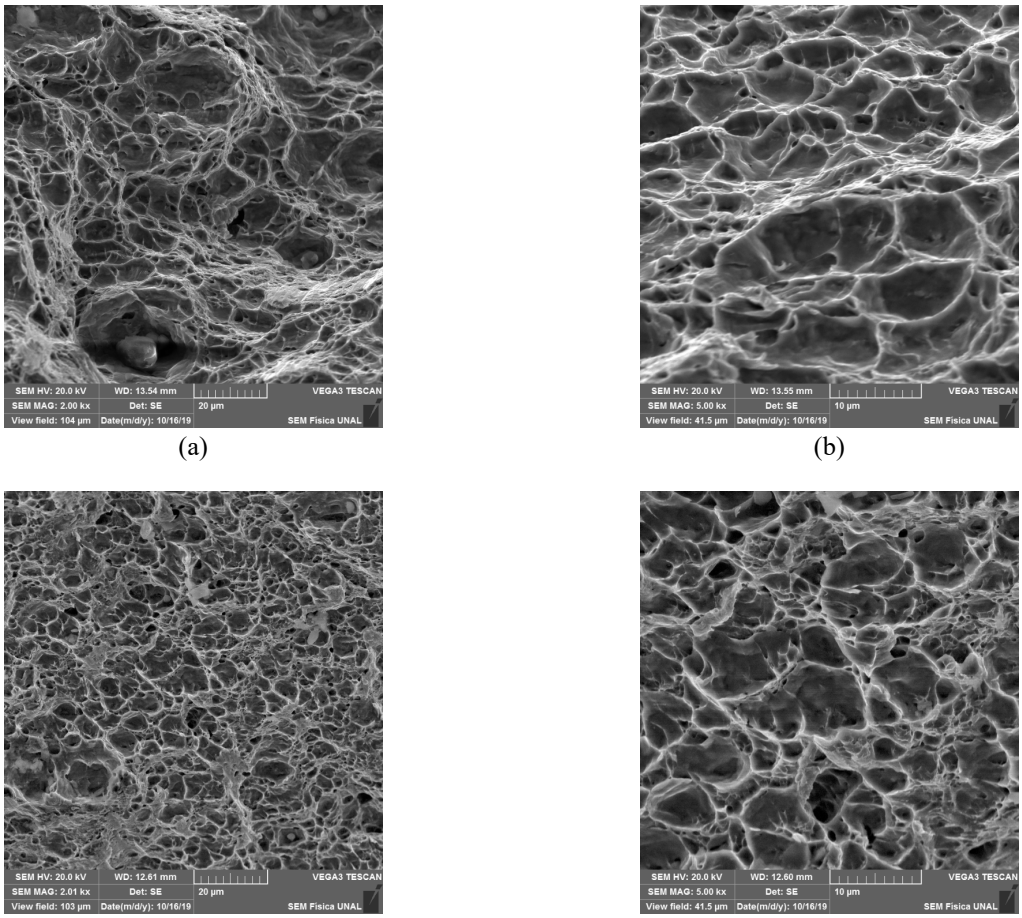

Figure 8. SEM fractography of fracture surface of (a),(b) as-received and (c),(d) heat-treated toughness test samples.

XFEM Simulation

Figures 9(a) and 9(b) show the load-displacement curves for fracture toughness test for AS and HT samples, respectively. The results show good concordance between the experimental and computational results. 1 mm size element was used for the simulations, due that this element size allows reaching convergence on the computational model. The results for a mesh with the element size of 1 mm shows that during the crack growth, the error of the computational model regarding experimental load-displacement curve achieved values between 1% and 15% (both for the as-received and heat-treated materials). Figure 10 shows the difference between the structured and unstructured meshes with a similar element size. Figure 10(a) shows the small difference between the two meshes for AR samples, a similar behaviour for the HT sample is displayed in Figure 11(b). Moreover, a slight difference is observed when the peak load is achieved for the HT sample, whereas for AR sample is higher, but with, a pretty good agreement is shown during the crack growth.

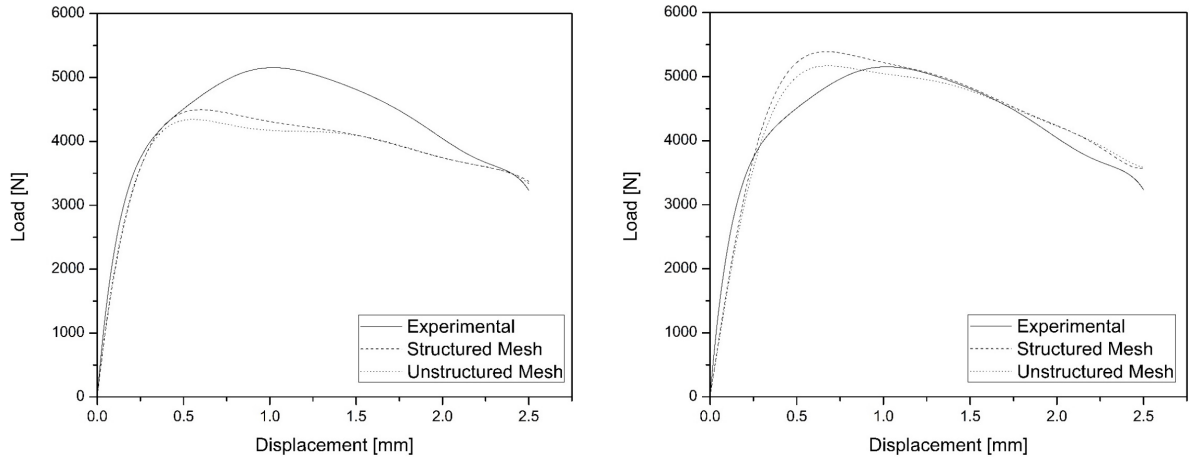

Figure 9. Comparison between experimental and computational load-displacement results for (a) as-received and, (b) heat-treated samples.

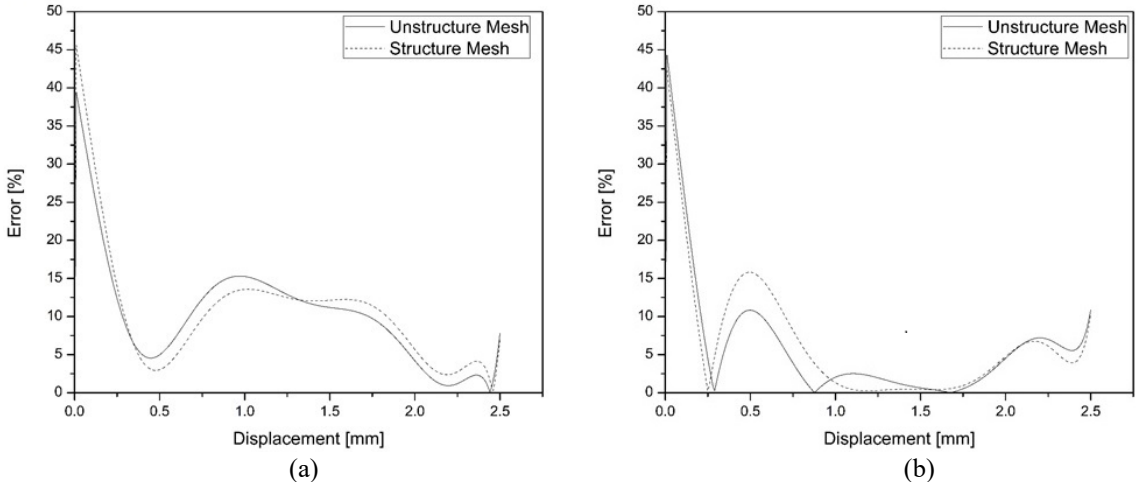

Figure 10. Computational model error regarding experimental load-displacement curve for (a) as-received and, (b) heat-treated samples.

CONCLUSION

It was possible to achieve an increase of martensite volume fraction in low-carbon dual-phase steel, with the implementation of heat treatment. The microstructure maintains its grain size and equiaxial compared with the as-received samples. The obtained results on the fatigue crack propagation test showed that after the heat treatment, the increment of martensite on the microstructure is effective to decelerate the crack propagation. The crack propagation is more difficult trough the martensite phase, due to generating a crack closure effect on the crack tip during the propagation.

The increase of the martensite phase in the dual-phase steel microstructure results in a slight increment on fracture toughness, due to plastic deformation difference between ferrite and martensite. The low carbon content in the martensite phase generates low values of hardness and more ductile behaviour, generating better compatibility between both phases. The load-displacement curves for as-received a heat treatment material obtained using the XFEM model showed a good agreement with the experimental data since the error for the two conditions is between 1% and 15%. Finally, there was no significant difference between the numerical results using structured and unstructured mesh. Higher content of

martensite in the dual-phase steel microstructure shows to be a good way to increase the fracture resistance under different load conditions, quasistatic and dynamic loads. The present work shows an increase of fracture toughness, tensile strength and fatigue resistance when the as-received material is heat-treated.

ACKNOWLEDGEMENT

The authors thank the financial support provided by Universidad Nacional de Colombia, as well as the support of laboratories from the Mechanical and Mechatronics Engineering Department on the development of this work.

REFERENCES

[1] Li Z, Wu D, Lü W, Yu H, Shao Z, Luo L. Effect of holding time on the microstructure and mechanical properties of dual-phase steel during intercritical annealing. Journal of Wuhan Univesity of Technology-Materials Science Edition 2015; 30(1): 156-161.

[2] Pouranvari M. Work hardening behavior of Fe-0.1 C dual phase steel. BHM Berg – und Hüettenmäennische Monatshefte 2012; 157(1): 44-47.

[3] Zhang J, Di H, Deng Y, Misra RDK. Materials Science & Engineering A Effect of martensite morphology and volume fraction on strain hardening and fracture behavior of martensite – ferrite dual phase steel. Materials Science and Engineering: A 2015; 627: 230-240.

[4] Ahmad E, Manzoor T, Ziai MMA, Hussain N. Effect of Martensite Morphology on Tensile Deformation of Dual-Phase Steel, Journal of Materials Engineering and Performance 2012; 21(3): 382-387.

[5] Avendaño Rodríguez D, Granados JD, Espejo Mora E, Mujica Roncery L, Rodríguez Baracaldo R. Fracture mechanisms in dual-phase steel: Influence of martensite volume fraction and ferrite grain size. Journal of Engineering Science and Technology Review 2018; 11(6): 174-181.

[6] Mazaheri Y, Kermanpur A, Najafizadeh A. A novel route for development of ultrahigh strength dual phase steels. Materials Science and Engineering: A 2015; 619: 1-11.

[7] de la Concepción VL, Lorusso HN, Svoboda HG. Effect of carbon content on microstructure and mechanical properties of dual phase steels. Procedia Materials Science 2015; 8: 1047-1056.

[8] Li S, Kang Y, Kuang S. Effects of microstructure on fatigue crack growth behavior in cold-rolled dual phase steels. Materials Science and Engineering: A 2014; 612: 153-161.

[9] Sudhakar K, Dwarakadasa E. A study on fatigue crack growth in dual phase martensitic steel in air environment. Bulletin of Materials Science 2000; 23(3): 193-199.

[10] Dutta VB, Suresh S, Ritchie RO. Fatigue crack propagation in dual-phase steels effects of ferritic-martensitic microstructures on crack path morphology. Metallurgical and Materials Transactions A 1984; 15: 1193-1207.

[11] Idris R, Abdullah S, Thamburaja P, Omar MZ. Entropy-based approach for fatigue crack growth rate of dual-phase steel. International Journal of Integrated Engineering 2018; 10(5): 1-7.

[12] Idris R, Prawoto Y. Influence of ferrite fraction within martensite matrix on fatigue crack propagation : An experimental verification with dual phase steel. Materials Science and Engineering: A 2012; 552: 547-554.

[13] Ulu S, Aytekin H, Said G. An alternative approach to the fracture toughness. Strength of Materials 2013; 45: 607-618.

[14] Chao YJ, Ward JD, Sands GR, Charpy impact energy, fracture toughness and ductile-brittle transition temperature of dual-phase 590 Steel. Materials & Deisgn 2007; 28(2): 551-557.

[15] Alaneme KK. Fracture toughness (K_{1C}) evaluation for dual phase medium carbon low alloy steels using circumferential notched tensile (CNT) Specimens. Materials Research 2011; 14(2): 155-160.

[16] Sarkar R, Chandra SK, De PS, Chakraborti PC, Ray SK. Evaluation of ductile tearing resistance of dual-phase DP 780 grade automotive steel sheet from essential work of fracture (EWF) tests. Theorical and Applied Fracture Mechanics 2019; 103: 102278.

[17] Casellas D, Lara A, Frometa D, et al. Fracture toughness to understand stretch-flangeability and edge cracking resistance in AHSS. Metallurgical and Materials Transactions A 2017; 48(1): 86-94.

[18] ASTM E1820-15a. Standard test method for measurement of fracture toughness. Annual book of ASTM standards, West Conshohocken, PA: American Society for Testing and Materials; 2015.

[19] Nikfam MR, Zeinoddini M, Aghebati F, Arghaei AA. Experimental and XFEM modelling of high cycle fatigue crack growth in steel welded T-joints. International Journal of Mechanical Sciences 2019; 153-154: 178-193.

[20] Cai W. Fracture simulation of structural steel at elevated temperature using XFEM technique. IOP Conference Series: Materials Science and Enginnering 2017; 264

[21] Zhang J, Kiekens C, Hertelé S, De Waele W. Identification and prediction of mixed-mode fatigue crack path in high strength low alloy steel. Proceedings 2018; 2(8): 504.

[22] Chang Y, Song Q, Kuang Z, Zhang K, Zhrng Z. Fracture analysis of cast iron materials with cracks based on elastoplastic extended finite element method. Acta Mechanica Solida Sinica 2019; 32(2): 201-214.

[23] Vajragupta N, Uthaisangsuk V, Schmaling B, Münstermann S, Hartmaier A, Bleck W. A micromechanical damage simulation of dual phase steels using XFEM. Computational Materials Science 2012; 54(1): 271–279.

[24] Ramazani A, Chang Y, Prahl U. Characterization and modeling of failure initiation in bainite-aided DP steel. Advanced Engineering Materials 2014; 16(11): 1370–1380.

[25] Sirinakorn T, Uthaisangsuk V. Investigation of damage initiation in high-strength dual-phase steels using cohesive zone model. International Journal Damage of Mechanics 2018; 27(3): 409–438.

[26] ASTME8/M8-16a – Standard test method for tension testing of metallic materials.Annual book of ASTM standards, West Conshohocken, PA: American Society for Testing and Materials; 2016.

[27] ASTM E647-15. Standard test method for measurement of fracture toughness. Annual book of ASTM standards, West Conshohocken, PA: American Society for Testing and Materials; 2015.

[28] Calcagnotto M, Adachi Y, Ponge D, Raabe D. Deformation and fracture mechanisms in fine- and ultrafine-grained ferrite / martensite dual-phase steels and the effect of aging. Acta Materalia 2011; 59(2): 658–670

[29] Saeidi N, Ashrafizadeh F, Niroumand B. Development of a new ultrafine grained dual phase steel and examination of the effect of grain size on tensile deformation behavior. Materials Science and Engineering: A 2014; 599: 145–149.

[30] Soliman M, Palkowski H. Tensile properties and bake hardening response of dual phase steels with varied martensite volume fraction. Materials Science and Engineering: A 2020; 777: 139044

[31] Balbi M, Alvarez-Armas I, Armas A. Effect of holding time at an intercritical temperature on the microstructure and tensile properties of a ferrite-martensite dual phase steel. Materials Science and Engineering: A 2018; 733: 1-8.

[32] Fonstein N. Dual-phase steels. In: Rana R, Singh B, editors. Automotive steels: design, metallurgy, processing and applications, Cambridge: Woodhead Publishing 2017, p 285-311.

[33] Mohanty JR, Verma BB, Ray PK. Determination of fatigue crack growth rate from experimental data: a new approach. International Journal of Microstructure and Materials Properties 2010; 5(1): 79.

[34] Al-Bakri AA, Sajuri Z, Abdulrazzaq M, Ariffin AK, Fafmin MS. Fatigue properties of strained very thin 304 stainless steel sheets. International Journal of Automotive and Mehcanical Engineering 2017; 14(2): 4171-4182.

[35] Laurito DF, Baptista CARP, Torres MAS, Abdalla AJ. Microstructural effects on fatigue crack growth behavior of a microalloyed steel. Procedia Engineering 2010; 2(1): 1915–1925.

[36] Akay SK, Yazici M, Bayram A, Avinc A, Fatigue life behaviour of the dual-phase low carbon steel sheets. Journal of Materials Processing Technology, 2009; 209(7): 3358-3365.

[37] Idris R, Abdullah S, Thamburaja P, and Omar MZ. An experimental investigation of tensile properties and fatigue crack growth behaviour for dual-phase steel. Journal of Mechanical Engineering 2018; 15(2): 155-167.

[38] Zhao A, Xie J, Sun C, Lei Z, Hong Y. Effects of strength level and loading frequency on very-high-cycle fatigue behavior for a bearing steel. International Journal of Fatigue 2012; 38: 46-56.

[39] Gou R, et al. Microstructure failure in ferrite-martensite dual phase steel under in-situ tensile test. Journal of Iron and Steel Research International 2017; 24(3): 350-356.

[40] Lai Q, Bouaziz O, Gouné M, Brassartd L,Verdiera M, Parrya G, Perladee A, Brécheta Y, Pardoend T. Damage and fracture of dual-phase steels: Influence of martensite volume fraction. Materials Science and Engineering: A 2015;646:322–331.

[41] Movahed P, Kolahgar S, Marashi SPH, Pouranvari M, Parvin N. The effect of intercritical heat treatment temperature on the tensile properties and work hardening behavior of ferrite-martensite dual phase steel sheets. Materials Science and Engineering: A 2009;518(1–2):1–6.

[42] Yoon JI, Jung J, Lee HH, Kim JY, Kim HS. Relationships between stretch-flangeability and microstructure-mechanical properties in ultra-high-strength dual-phase steels. Metals and Materials International 2019; 25(5): 1161-1169.

[43] Zheng X, Ghassemi-Armaki H, Srivastava A. Structural and microstructural influence on deformation and fracture of dual-phase steels. Materials Science and Engineering: A 2019; 774: 138924.

[44] Sun Y, Li X, Yu X, Ge D, Chen J, Chen J, Fracture morphologies of advanced high strength steel during deformation. Acta Metallurgica Sinicia (English Letters) 2014; 27: 101-106.